

Article

Efficient 5.8 GHz Microstrip Antennas for Intelligent Transportation Systems: Design, Fabrication, and Performance Analysis

Muhammet Tahir Guneser ^{1,*}, Cihat Seker ¹, Mehmet Izzeddin Guler ², Norma Latif Fitriyani ³ and Muhammad Syafrudin ^{3,*}

¹ Department of Electrical and Electronics Engineering, Karabuk University, Karabuk 78050, Turkey; cihatseker@karabuk.edu.tr

² Department of Mechatronics Engineering, Karabuk University, Karabuk 78050, Turkey; izzeddin@karabuk.edu.tr

³ Department of Artificial Intelligence and Data Science, Sejong University, Seoul 05006, Republic of Korea

* Correspondence: mtguneser@karabuk.edu.tr (M.T.G.); udin@sejong.ac.kr (M.S.)

Abstract: In this study, we designed a high-performance, compact E-shaped microstrip antenna optimized for intelligent transportation systems, operating at 5.8 GHz. Utilizing simulation tools such as CST Studio Suite 2022 Learning Edition, Ansys HFSS 2022 R1, and MATLAB 2022b PCB Antenna Designer, we ensured consistent physical parameters. Fabricated with a 1.6 mm thick FR-4 substrate and a 50 Ω microstrip line-feeding technique, the antenna measures $35 \times 50 \times 1.6$ mm³, smaller than already existing designs. At 5.75 GHz, it exhibits a return loss of -23.68 dB and a VSWR of 1.140 dB, ensuring stable performance within the desired frequency band. Our findings recommend its integration into vehicle-to-infrastructure wireless communication systems. Comparison across simulation environments and laboratory measurements highlights the close alignment of results with those from Ansys HFSS 2022 R1, affirming its reliability.

Keywords: e-shaped antenna; microstrip antenna; intelligent transportation systems; 5.8 GHz band; design optimization; performance analysis

MSC: 78A50; 90C08



Citation: Guneser, M.T.; Seker, C.; Guler, M.I.; Fitriyani, N.L.; Syafrudin, M. Efficient 5.8 GHz Microstrip Antennas for Intelligent Transportation Systems: Design, Fabrication, and Performance Analysis. *Mathematics* **2024**, *12*, 1202. <https://doi.org/10.3390/math12081202>

Academic Editor: Carlos Conceicao Antonio

Received: 6 March 2024

Revised: 30 March 2024

Accepted: 4 April 2024

Published: 17 April 2024



Copyright: © 2024 by the authors. Licensee MDPI, Basel, Switzerland. This article is an open access article distributed under the terms and conditions of the Creative Commons Attribution (CC BY) license (<https://creativecommons.org/licenses/by/4.0/>).

1. Introduction

The burgeoning diversity of modern wireless communication systems and their pervasive integration into biomedical applications have significantly heightened the demand for antennas suitable for seamless integration into portable devices. As users increasingly seek ubiquitous access to data, the miniaturization of antennas in portable devices has become imperative, driving a surge in interest in microstrip technology. Consequently, there is a pressing need for antennas capable of transmitting and receiving signals in a smaller and lighter form factor [1]. The performance of microstrip antennas exhibits considerable variability based on factors such as the dielectric substrate [2], size, and geometry [3,4]. The resonance frequency, polarization, radiation pattern, and impedance matching of a microstrip antenna can all fluctuate depending on the selected patch geometry [5]. While the literature overflows with various geometries accompanied by their respective design equations, including rectangular, circular, elliptical, square, triangular, polygonal, and nature-inspired shapes [6–11], some antenna configurations lack a comprehensive technical design methodology. Design equations for these configurations are either absent in the literature [12–16] or constrained due to variations in dielectric permittivity [17]. Given the critical importance of accurately determining resonance frequency to mitigate co-channel and adjacent channel interference as well as the associated complications [18], this paper proposes and presents novel mathematical models to address these challenges. An antenna serves as a pivotal wireless system element, facilitating communication by

enabling the transfer of data between transmitter and receiver through the propagation of electromagnetic energy.

The evolution of wireless communication from its inception with first-generation (1G) systems to the latest 5G networks in 2022 marks a profound technological journey [1,2]. IEEE-defined wireless network standards encompass a diverse array of protocols, with WLAN protocols grounded in the IEEE 802.11 standard [19], colloquially referred to as “Wi-Fi”. This standard encompasses a spectrum of protocols, including 802.11a, 802.11b, 802.11g, and 802.11n [3]. Intelligent transportation systems (ITS) are delineated within the IEEE 802.11p standard [19], operating within the 5.850–5.925 GHz frequency band with a bandwidth of 100 MHz. The utilization of this band range, in ITS [4], is geared towards averting accidents, mitigating traffic congestion, and ameliorating other adverse impacts. By harnessing this band range, vehicles can operate with enhanced safety, synchronization, and efficiency [5,6].

As the proliferation of minimalist technological devices continues unabated, the demand for smaller, high-bandwidth, multiband antennas capable of facilitating simultaneous communication among the myriad of devices in wireless networks is escalating [7]. Microstrip antennas, characterized by their diminutive stature, lightweight nature, ease of integration, and cost-effectiveness, emerge as a quintessential choice for antenna design applications. Comprising a flat metallic region known as a patch, a dielectric substrate, a ground plane, and a feeding source, microstrip antennas exemplify versatility and versatility [8,9]. They reign supreme as the preferred antenna type across a spectrum of cutting-edge technologies, including RFID, cell phones, WLAN, Wi-Fi, WiMax, and GPS systems. Leveraging parameters such as dimensional properties, dielectric materials, and feeding methodologies, engineers can tailor microstrip antennas to meet diverse application requirements with unparalleled precision.

However, microstrip antennas are not without their limitations, notably, their restricted bandwidth [10]. Mitigating this constraint necessitates strategic interventions, such as altering the substrate thickness to broaden the bandwidth [11]. Furthermore, techniques like perforating the patch, inducing parasitic elements through scraping, employing E/H-shaped patches, and adopting various feeding shapes have been instrumental in augmenting the bandwidth [12]. Similarly, incorporating parasitic elements and implementing scraping on the ground plane have proven efficacious in attaining the desired gain and bandwidth parameters [13,14].

Among the myriad of feeding methods employed in microstrip antennas, four stand out as particularly prevalent: microstrip feed, coaxial feed, aperture-coupled feed, and proximity-coupled feed [15]. Microstrip feed, distinguished by its simplicity of manufacture, ease of positioning determination, and straightforward modeling, enjoys widespread favor among antenna designers [16].

In the landscape of microstrip antenna research, notable contributions have been made by various scholars employing diverse simulation environments and substrates. In 2020, Silalahi et al. engineered a microstrip antenna with a commendable bandwidth of 1.02 GHz, centered at 5.8 GHz on an FR-4 plate, tailored for Wi-Fi applications, utilizing the CST Studio Suite 2011 simulation environment [17]. Similarly, in 2019, C. Divya et al. harnessed the CST Studio Suite simulation environment to fashion an antenna on an FR-4 substrate, achieving a bandwidth of approximately 100 MHz suited for industrial, scientific, and medical (ISM) applications [18]. Meanwhile, in 2021, Akash Modi et al. delved into the realm of microstrip antenna design, leveraging the Ansys HFSS simulation environment to scrutinize an antenna crafted on a Rogers RT/Duroid5880 substrate, yielding a noteworthy bandwidth of 2.17 GHz within the 5.8 GHz band [20]. Moreover, Bathula Lakshmi Narayana et al. (2015) pioneered the development of a multiband antenna on the Rogers/RT Duroid 5870 substrate, showcasing a bandwidth of approximately 10 MHz centered at 5.8 GHz [21].

Other notable endeavors include the work of Younes El Hachimi et al. in 2018, focusing on an antenna tailored for RFID reader applications [22], and Sayed Amirul Hassan et al.'s 2017 exploration of an antenna designed for Internet of Things (IoT) applications [23].

Notably, the latter half of 2021 witnessed the advent of the MATLAB PCB Antenna Designer Toolbox R2021b version, facilitating the design of microstrip antennas within the MATLAB simulation environment. This development opened new avenues for antenna design and analysis, as exemplified by the work of Khatri Kumar et al. in 2022, showcasing the efficacy of the MATLAB PCB Antenna Designer Toolbox R2021b version [24].

Despite these advancements, a notable gap exists in the literature concerning comparative studies across different simulation platforms such as CST Studio Suite, Ansys HFSS, and the MATLAB PCB Antenna Designer software [25–27].

In this study, we employ a microstrip feed in our proposed antenna design, employing a rectangular patch measuring 5×8 to the ground plane to achieve a center frequency of 5.8 GHz. We meticulously compare the return losses (S_{11}), voltage standing wave ratio (VSWR), and gain analyses across the three software platforms, shedding light on their respective strengths and limitations in antenna design and analysis.

In summary, our study contributes to the field by designing a compact microstrip antenna for intelligent transportation systems, comparing simulation results from CST Studio Suite 2022 Learning Edition, Ansys HFSS 2022 R1, and MATLAB R2022b PCB Antenna Designer, identifying the closest simulation environment to the produced antenna's performance, analyzing impedance-matching capabilities, and suggesting avenues for future research.

2. Antenna Design

The calculation steps for determining the physical parameters of the microstrip antenna, meticulously tailored in the CST Studio Suite 2022 Learning Edition, Ansys HFSS 2022 R1, and MATLAB R2022b PCB Antenna Designer simulation environments, are succinctly outlined in Figure 1. Figure 1 serves as a comprehensive guide, delineating each crucial step involved in the derivation of the antenna's geometric structure, as elucidated in Table 1. This meticulous approach ensures precision and consistency across all simulation platforms, facilitating a rigorous analysis and comparison of the antenna's performance metrics.

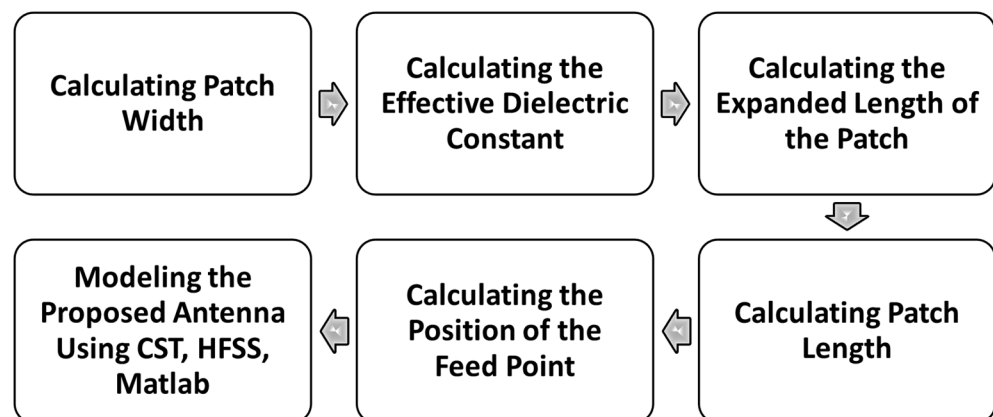


Figure 1. The design steps of the e-shaped antenna in a simulation environment.

The detailed geometric configuration of the antenna is depicted in Figures 2 and 3, meticulously adhering to the dimensions specified in Table 2, with all the measurements provided in millimeters. Furthermore, Figure 4 showcases the physical prototype of the antenna, fabricated using the LPKF Protomat s62 device. The antenna presented in this report boasts dimensions of $35 \times 50 \times 1.6$ mm and utilizes the FR-4 material as the substrate, renowned for its dielectric constant ($\epsilon_r = 4.3$). A conductor with a thickness of 0.035 mm, crafted from copper, is employed in the antenna's construction. Additionally, a 50Ω microstrip feed line is incorporated as the antenna's feed, ensuring optimal performance. The introduction of two slots in the patch component of the antenna serves to fine-tune its operation at the center frequency of 5.8 GHz.

Table 1. The mathematical model of the e-shaped antenna.

$f_r(\text{GHz})$: Operating Frequency
ϵ_r	: Dielectric Constant
Step 1	: To calculate patch width
$W = \frac{v_0}{2f_r} \sqrt{\frac{2}{\epsilon_r + 1}}$	
Step 2	: Effective Dielectric Constant
$\epsilon_{reff} = \frac{\epsilon_r + 1}{2} + \frac{\epsilon_r - 1}{2} \frac{1}{\sqrt{1 + 12 \frac{h}{W}}}$ $\frac{W}{h} > 1$	
Step 3	: Extended length of the patch
$\Delta L = 0.412 h \frac{(\epsilon_{reff} + 0.3)(\frac{W}{h} + 0.264)}{(\epsilon_{reff} - 0.258)(\frac{W}{h} + 0.8)}$	
Step 4	: To calculate the length of the patch
$L = \frac{v_0}{2f_r \sqrt{\epsilon_{reff}}} - 2\Delta$	

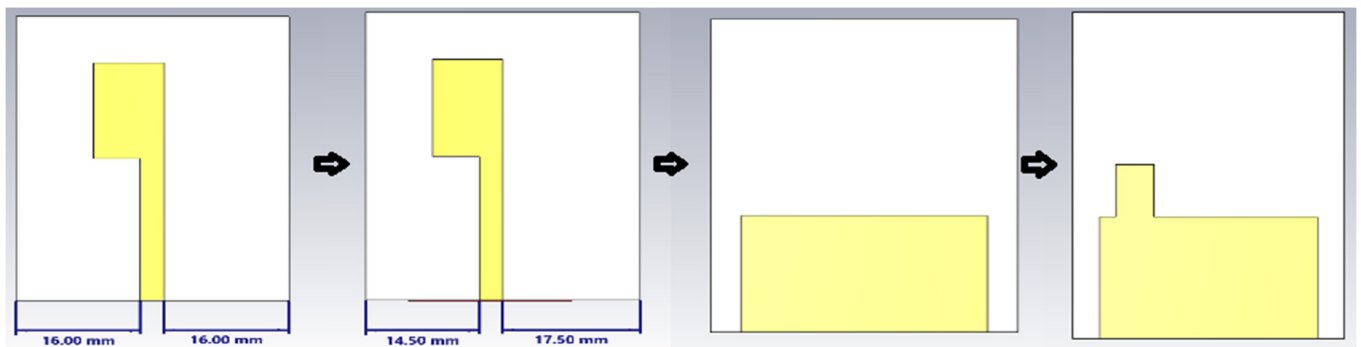


Figure 2. Designing process of the proposed antenna.

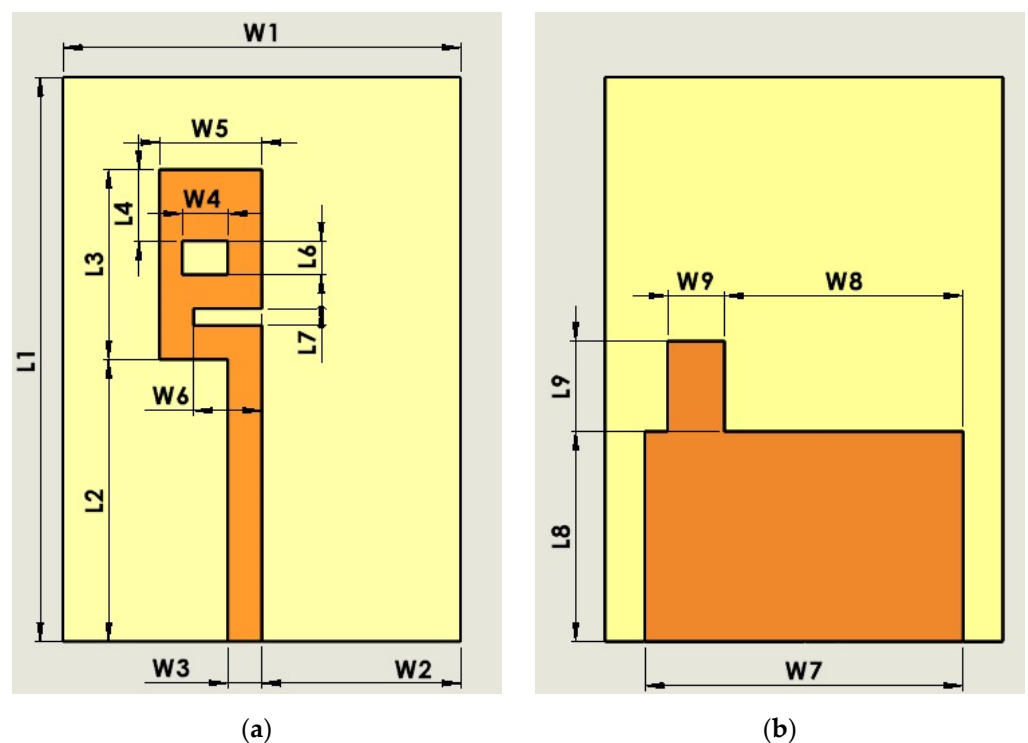
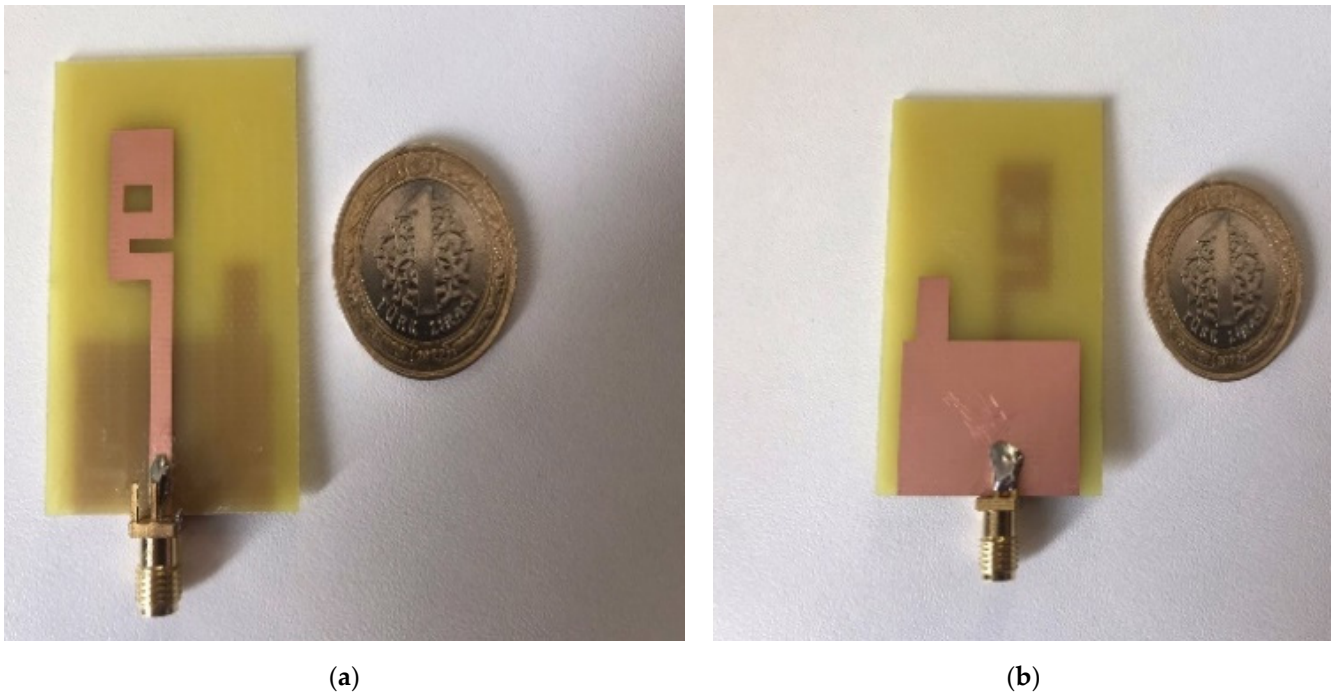


Figure 3. E-shaped antenna designed in the simulation environments: (a) top view, (b) bottom view.

Table 2. The geometric structure of the e-shaped antenna.

$W_1 = 35$	$W_6 = 6$	$L_2 = 25$	$L_8 = 18.6$
$W_2 = 17.5$	$W_7 = 28$	$L_3 = 16.8$	$L_9 = 8$
$W_3 = 3$	$W_8 = 21$	$L_4 = 6.3$	
$W_4 = 4$	$W_9 = 5$	$L_6 = 3$	
$W_5 = 9$	$L_1 = 50$	$L_7 = 1.5$	

**Figure 4.** E-shaped antenna produced with LPKF Protomat s62: (a) top view, (b) bottom view.

In the design and analysis of the antenna, we harnessed the capabilities of CST Studio Suite 2022 Learning Edition, Ansys HFSS 2022 R1, and MATLAB R2022b PCB Antenna Designer, leveraging their respective functionalities to meticulously scrutinize and optimize the antenna's performance. The results obtained from these simulations were meticulously compared with the physical prototype of the antenna, facilitating a comprehensive assessment of their accuracy and efficacy.

Following the intricate design stages delineated in Figure 3, the initial S_{11} value of -9.32 dB experienced a remarkable enhancement, plummeting to an impressive -23.68 dB in the final iteration. This substantial improvement underscores the efficacy of the design refinements implemented throughout the iterative optimization process. Such a noteworthy reduction in S_{11} not only signifies enhanced impedance matching but also reflects the meticulous attention to detail and relentless pursuit of optimal antenna performance throughout the design iterations.

3. Research Findings and Discussion

Indeed, CST Studio Suite, Ansys HFSS, and MATLAB PCB Antenna Designer stand as high-performance electromagnetic solvers revered for their prowess in designing, analyzing, and optimizing RF components and systems. Utilizing sophisticated computational algorithms, these state-of-the-art programs efficiently calculate essential antenna parameters such as the reflection coefficient, gain, bandwidth, and the voltage standing wave ratio (VSWR). By harnessing sophisticated techniques such as finite differences and the finite element method, these platforms empower engineers and researchers to meticulously model

electromagnetic phenomena, unravel intricate antenna behaviors, and fine-tune designs for an optimal performance. Their versatility and robust capabilities make them indispensable tools in the arsenal of antenna designers, facilitating the realization of innovative and high-performance RF solutions across a myriad of applications.

3.1. Return Loss (S_{11})

Return loss is a critical parameter in antenna applications, serving as a measure of how much power applied to the input port is reflected. It plays a pivotal role in assessing input port impedance mismatch and determining the operating frequency range of the antenna [28]. In our study, the antennas designed in different simulation environments exhibit distinct bandwidths and center frequencies. Specifically, the antenna crafted in CST Studio Suite 2022 Learning Edition boasts a bandwidth of 650 MHz, centered at 5.8 GHz, while its counterpart in Ansys HFSS 2022 R1 showcases a bandwidth of 600 MHz, with a center frequency of 5.8 GHz. Meanwhile, the antenna fashioned in MATLAB 2022b PCB Antenna Designer features a bandwidth of 500 MHz, centered at 5.8 GHz. In contrast, the produced antenna, subjected to measurements using the Vector Network Analyzer (VNA) of the Rohde & Schwarz Znh26 brand, depicted in Figure 5, demonstrates a bandwidth of 550 MHz and a center frequency of 5.8 GHz.



Figure 5. Return loss measurement of an e-shaped antenna using VNA.

The comparison of the antennas designed in the three simulation environments with the produced antenna, as illustrated in Figure 6, reveals that the results obtained from Ansys HFSS closely align with those of the produced antenna. This indicates that Ansys HFSS 2022 R1 yields the most accurate simulation results, closely matching the real-world performance of the antenna.

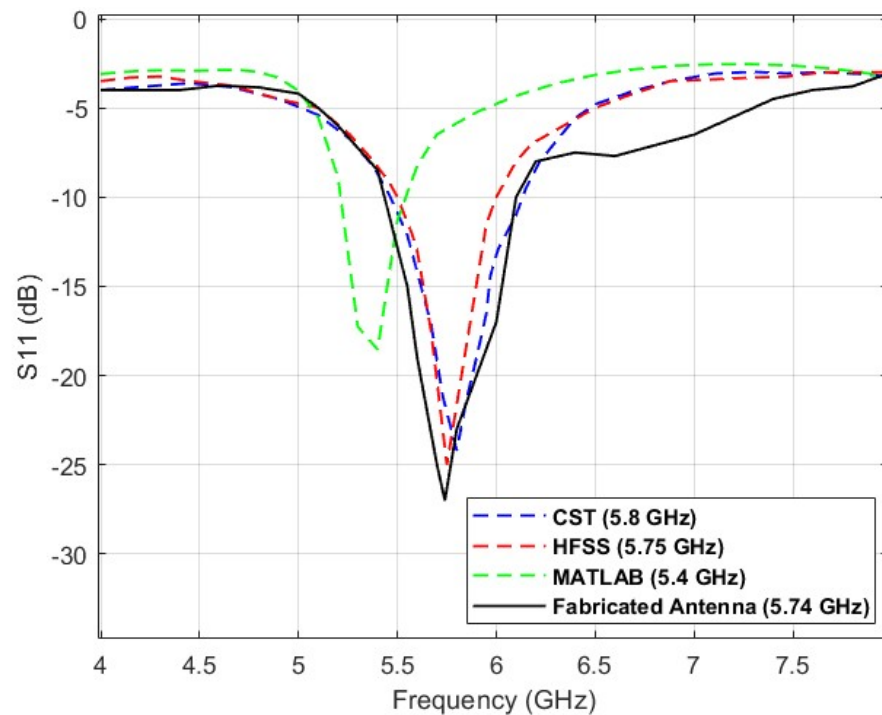


Figure 6. Return loss of e-shaped antenna in simulation environments and laboratory measurement.

3.2. Radiation Pattern and Gain

The radiation pattern of a microstrip patch antenna characterizes how the antenna radiates electromagnetic waves into space. It depicts the amount of power radiated by the antenna at different angles and determines important characteristics of the antenna such as directivity, gain, and efficiency. Gain measures the antenna's ability to concentrate energy in a particular direction, thus indicating its effectiveness in communication systems. The gain of an antenna is typically expressed in decibels (dB). The results garnered from the CST Studio Suite 2022 Learning Edition, Ansys HFSS 2022 R1, and MATLAB 2022b PCB Antenna Designer programs for radiation pattern and gain are delineated in Figures 7–9, respectively, providing insights into the anticipated performance of the designed antennas. Contrastingly, Figure 10 illustrates the measured gain of the antenna, captured during testing within the anechoic chamber, as depicted in Figure 11. The proposed antenna was placed on a rotating turntable. A horn antenna was used as the receiving antenna due to its high gain. The VNA was calibrated. The S-parameters of the antenna were measured at different frequencies using the VNA. The gain of the antenna was calculated using the measured S-parameters. The measurement was repeated by rotating the proposed antenna at different angles. The gain of the manufactured antenna was 1.98 dBi.

The 3D gain plot depicts the magnitude of the electric field in the far-field region of the antenna. The radiation pattern, on the other hand, illustrates the direction and magnitude of the Poynting vector in the far-field region. The Poynting vector represents the energy flow of electromagnetic waves. Consequently, the gain plot and radiation pattern are also interconnected and exhibit similar patterns. Three simulation environments yielded distinct results for both the radiation pattern and the gain. Upon the examination of the antenna's radiation pattern plots, discrepancies were observed in the three environments. For instance, the half-power beamwidth (HPBW) of the radiation patterns obtained in CST Studio Suite 2022 Learning Edition and Ansys HFSS 2022 R1 was approximately 48 degrees, whereas the HPBW of the radiation pattern obtained in MATLAB 2022b PCB Antenna Designer was greater than 48 degrees. Similarly, an analysis of the 3D gain plots of the antenna revealed variations across the three environments. For example, the maximum gain values obtained in CST Studio Suite 2022 Learning Edition and MATLAB 2022b PCB Antenna Designer were comparable, whereas the maximum gain value obtained in Ansys

HFSS 2022 R1 was slightly higher than the others. These inconsistencies can be attributed to minor discrepancies in the employed simulation algorithms and modeling parameters.

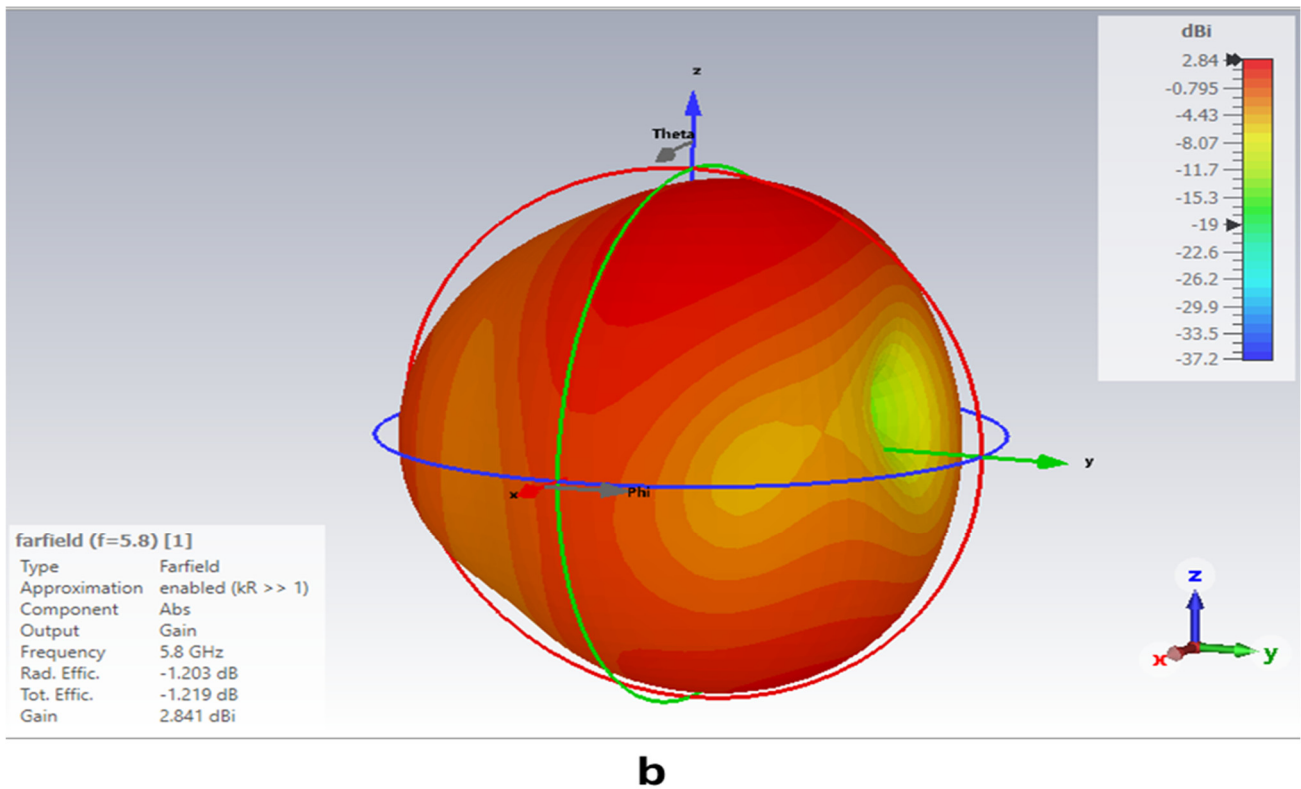
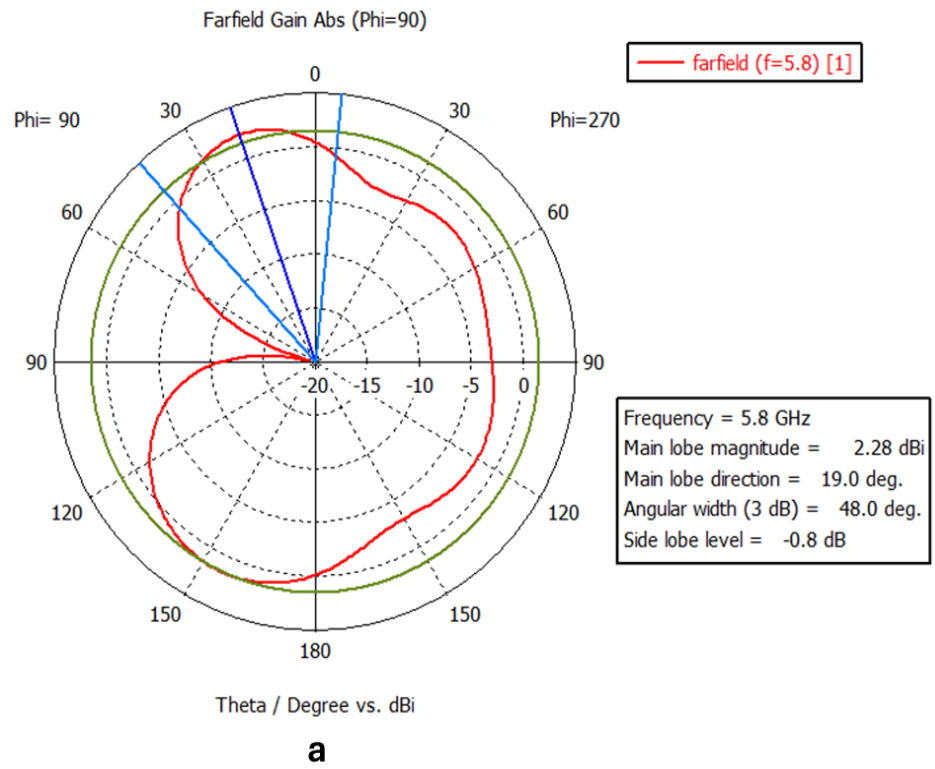


Figure 7. (a) Radiation pattern and (b) 3D gain of the e-shaped antenna in the CST Studio Suite 2022 Learning Edition environment.

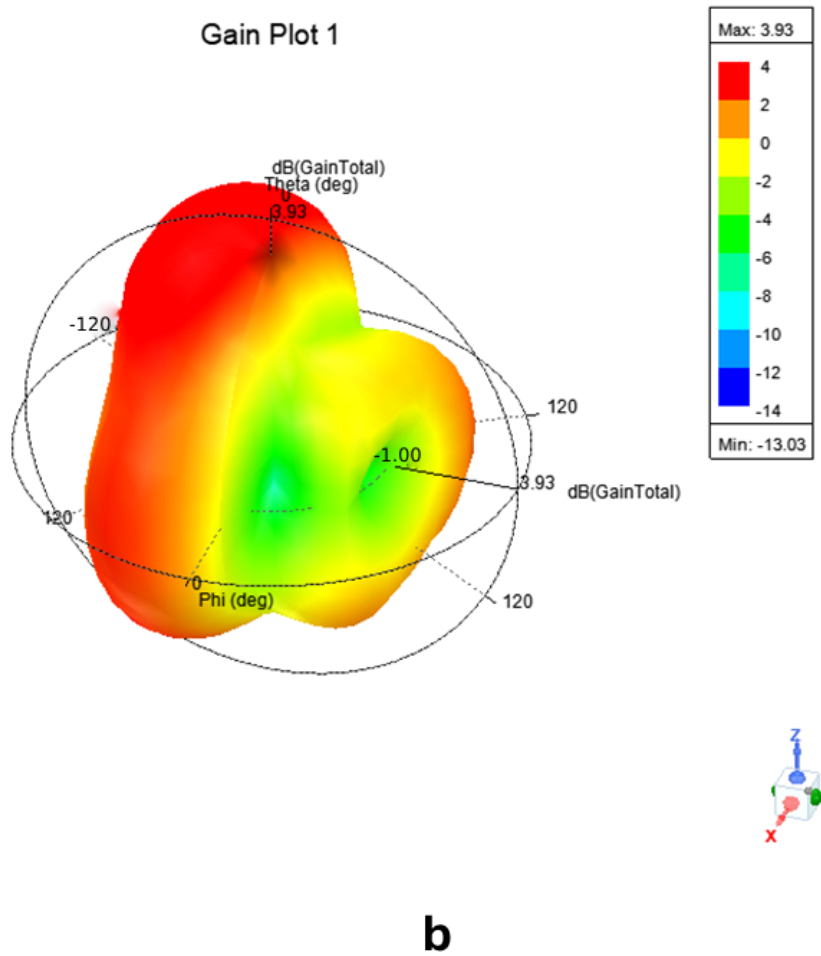
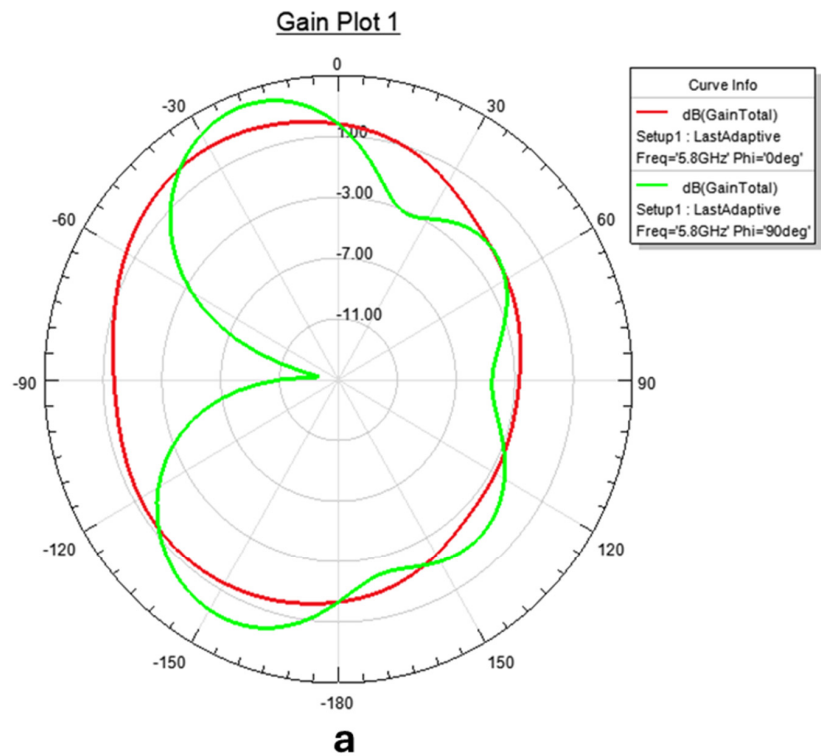
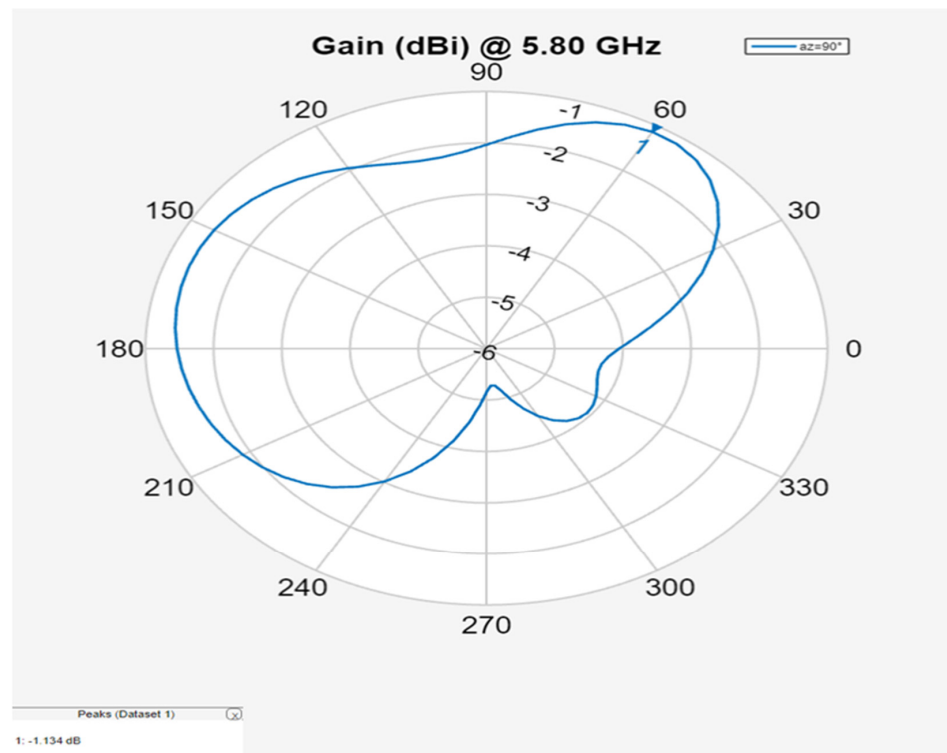
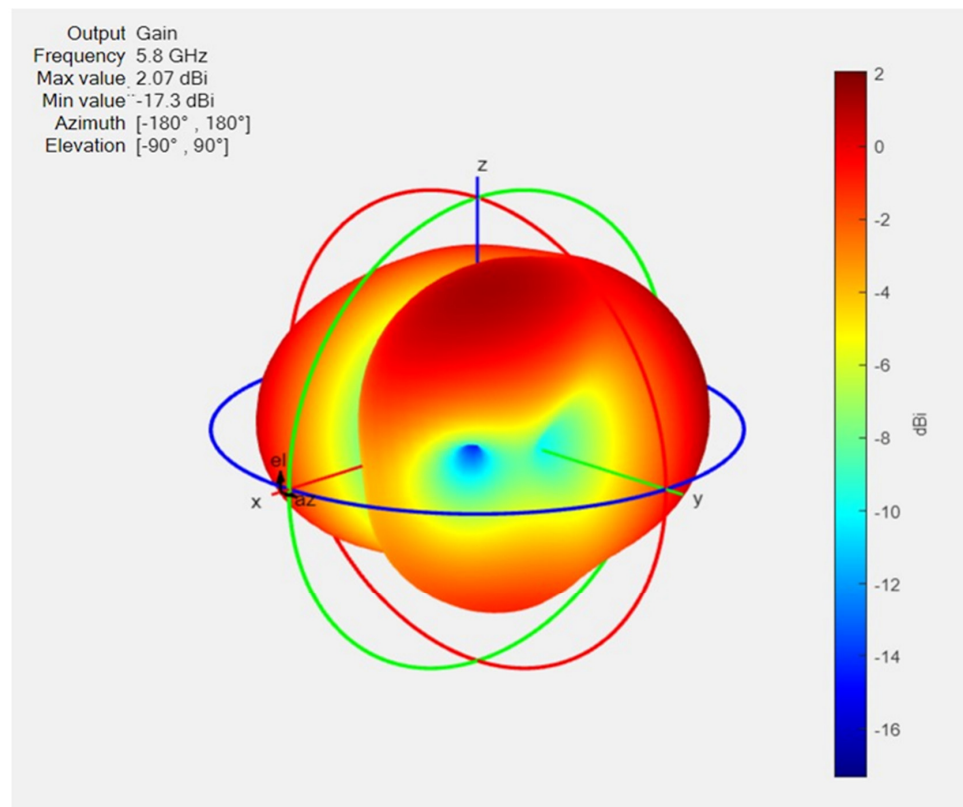


Figure 8. (a) Radiation pattern and (b) 3D gain of the e-shaped antenna in the Ansys HFSS 2022 R1 environment.



a



b

Figure 9. (a) Radiation pattern and (b) 3D gain of the e-shaped antenna in the MATLAB 2022b PCB Antenna Designer environment.

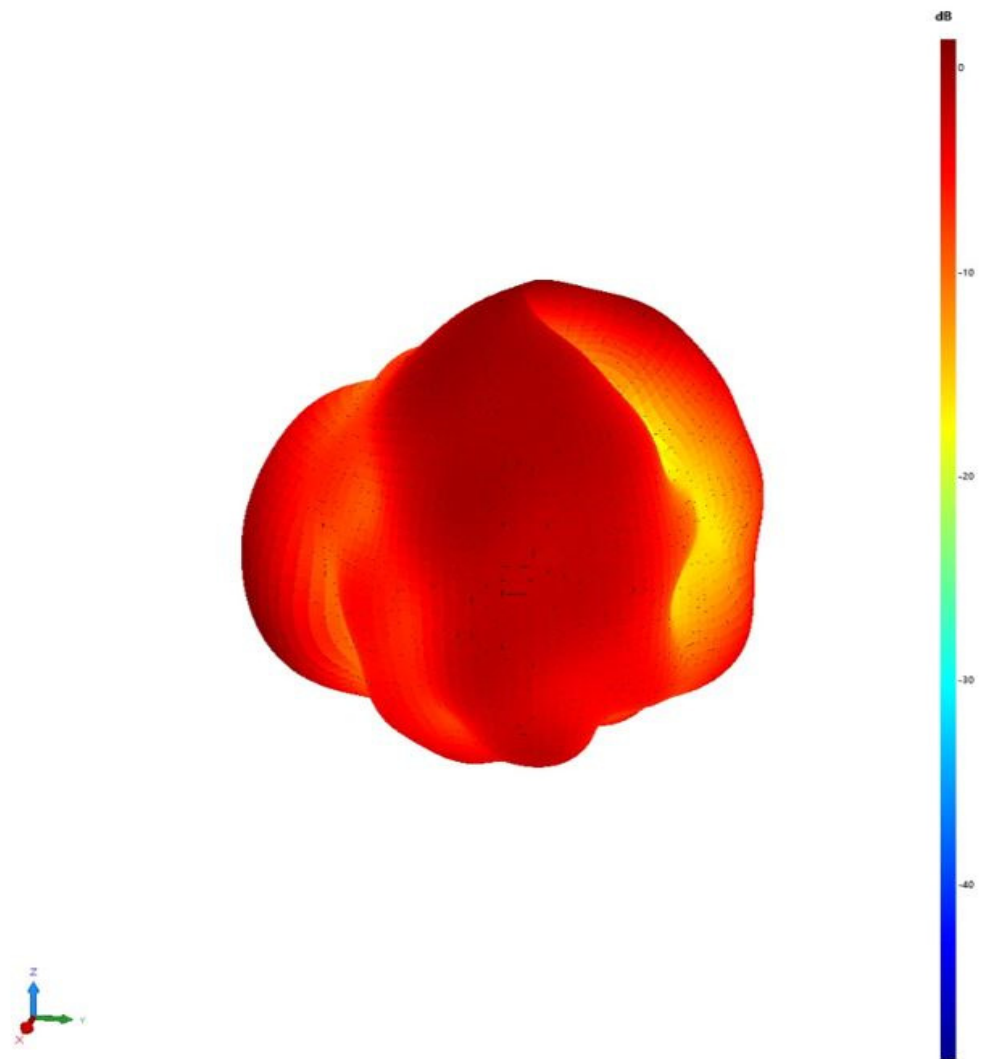


Figure 10. 3D gain of the e-shaped antenna in a laboratory measurement.

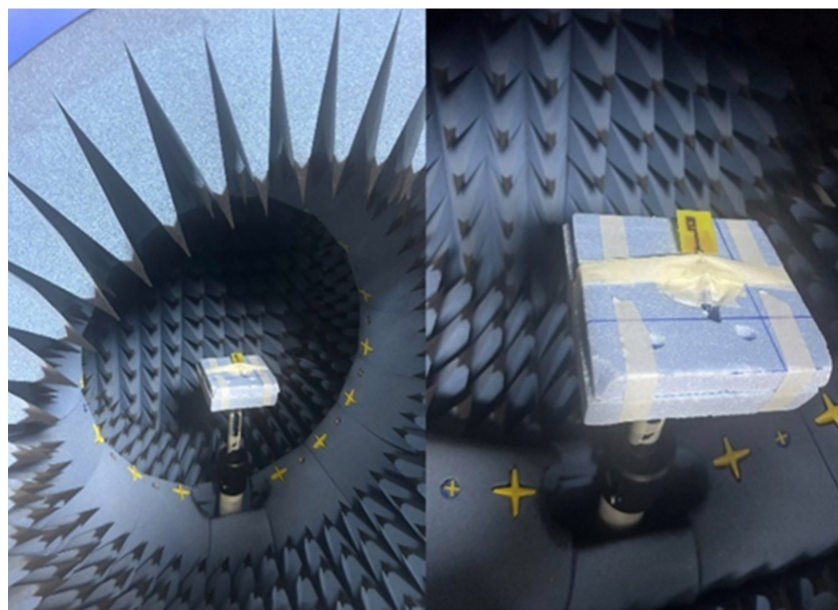


Figure 11. Measurement setup to determine the 3D gain of an e-shaped antenna.

The measured radiation efficiency of the proposed antenna was 86.2% in Ansys HFSS 2022 R1, 76.5% in CST Studio Suite 2022 Learning Edition, and 74.7% in the MATLAB 2022b PCB antenna designer. Upon a comparative analysis of the outcomes across the three software environments, MATLAB 2022b PCB Antenna Designer gave the closest result to the proposed antenna. This observation underscores the superior accuracy and fidelity of MATLAB 2022b PCB Antenna Designer in predicting antenna performance, thereby affirming its status as a preferred choice for antenna design and analysis endeavors.

3.3. Voltage Standing Wave Ratio (VSWR)

VSWR, or the voltage standing wave ratio, serves as a crucial indicator of the degree of impedance matching between an antenna's input impedance and the impedance of the transmission line. It is expressed as the ratio of the maximum to the minimum voltage on a transmission line, with values closer to 1 indicating better impedance matching [29].

In our study, the measurements of the produced antenna using the Vector Network Analyzer (VNA) of the Rohde & Schwarz Znh26 brand, depicted in Figure 12, yielded a VSWR value of 1.140. The VSWR results obtained from CST Studio Suite 2022 Learning Edition and Ansys HFSS 2022 R1 were 1.130 and 0.968, respectively. Unfortunately, VSWR measurements cannot be directly made in MATLAB 2022b PCB Antenna Designer. However, it is noteworthy that CST Studio Suite 2022 Learning Edition yielded the closest VSWR measurement to the produced antenna, highlighting its accuracy in predicting impedance matching.

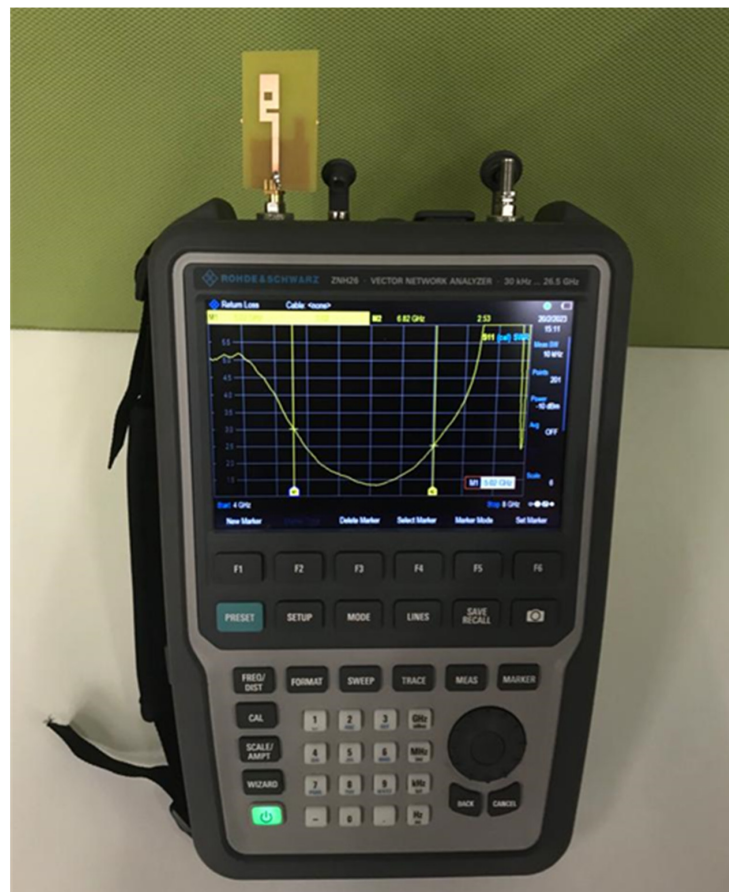


Figure 12. VSWR measurement of e-shaped antenna using VNA.

Figure 13 illustrates the comparison of the VSWR values of the antenna across its operating frequency range, showcasing the performance of the antenna in terms of impedance matching as predicted by the simulation environments.

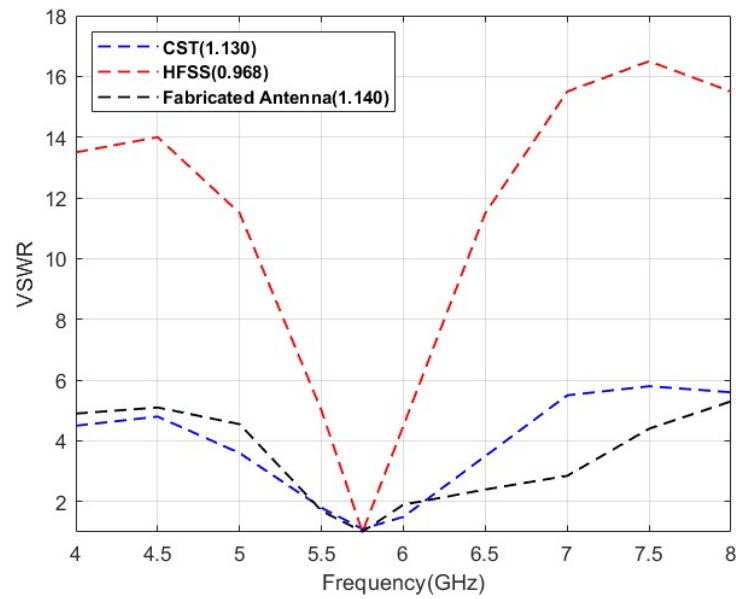


Figure 13. VSWR of the e-shaped antenna in simulation environments and laboratory measurements.

3.4. Comparison with Previous Works

Table 3 presents a comprehensive comparison of the dimensions, bandwidth, and gain values of the proposed antenna alongside antennas designed to operate within the 5.8 GHz band, as documented in references [30–38]. Notably, the gain value of the proposed antenna, as simulated in the simulation environment, surpasses that of the other antennas. Furthermore, the proposed antenna exhibits a notably high bandwidth compared to its counterparts. These findings underscore the exceptional performance and superior characteristics of the proposed antenna, positioning it as a compelling choice for applications requiring operation within the 5.8 GHz frequency band.

Table 3. Comparison of the proposed e-shaped antenna with other antennas in the literature.

Antenna	Dimension	Frequency Band (GHz) and Bandwidth (MHz)	Gain (dB)
[30]	36 × 32 × 1.6 FR-4	5.75 (740)	1.45
[31]	54.44 × 70.7 × 1.6 FR-4	5.8 (410)	2.21
[17]	50 × 50 × 1.6 FR-4	5.8 (770)	3.57
[32]	21.5 × 15 × 1.6 FR-4	5.71 (570)	2.45
[33]	17 × 18 × 0.8 FR-4	5.8 (150)	1.84
[34]	30 × 45 × 3.2 FR-4	5.8 (160)	1.59
[35]	19 × 19 × 0.76 Neltec	5.8 (≤200)	3.1
[36]	60 × 50 × 1.6 FR-4	5.81 (196)	3
[37]	91.5 × 30 × 0.1 Rogers 3850	5.9 (440)	1.6
[38]	31.76 × 34.39 × 2.03 FR-4	5.9 (More than one design)	(More than one design)
Proposed Antenna	35 × 50 × 1.6 FR-4	5.8 (550)	3.93

4. Conclusions

In this study, a compact and cost-effective microstrip antenna was meticulously designed for utilization in intelligent transportation systems, operating within the sub-6GHz band with a central frequency of 5.8 GHz. The proposed antenna model underwent a rigorous analysis in the CST Studio Suite 2022 Learning Edition, Ansys HFSS 2022 R1, and MATLAB 2022b PCB Antenna Designer simulation environments. This study presented a comprehensive comparison of three widely used simulation environments for the analysis of microstrip antennas. The aim was to determine which simulation environment produces the results closest to reality. In this respect, it is an important resource for antenna engineers and a foundation for future research. Key performance metrics such as return loss (S_{11}), gain, and the voltage standing wave ratio (VSWR) were scrutinized and compared across the three platforms. Notably, it was observed that the results obtained from the Ansys HFSS 2022 R1 simulation environment closely mirrored the performance of the produced antenna in terms of gain, whereas CST Studio Suite 2022 Learning Edition yielded results most closely resembling the VSWR measurements of the produced antenna. Although MATLAB 2022b PCB Antenna Designer software exhibited some inconsistencies in its analysis results, its integration capability with other toolboxes presents a notable advantage.

Furthermore, to fine-tune the antenna's performance, scraping was strategically employed in regions devoid of surface currents on the ground plane. This optimization technique facilitated the attainment of the desired center frequency and facilitated an increase in bandwidth [39]. The proposed antenna, featuring an FR-4 substrate with a thickness of 1.6 mm, boasts a bandwidth of 550 MHz and a remarkable -23.68 dB return loss at the center frequency of 5.75 GHz. Additionally, the measured VSWR value of 1.140 underscores the impedance-matching prowess of the antenna, further solidifying its stable and reliable performance compared to alternative designs. The antenna designed and fabricated in this study is ideal for ITS applications due to its small size, light weight, and low cost. The proposed antenna can be used in V2V and V2I communication, automatic toll collection, and automatic access control applications.

The limitations of our study include the inconsistencies observed in the analysis results from the MATLAB 2022b PCB Antenna Designer software and potential variations in performance under different environmental conditions. Future works may focus on further optimizing the antenna's design to enhance its performance metrics and exploring novel materials and manufacturing techniques to reduce costs and improve efficiency.

Author Contributions: Conceptualization, M.T.G. and M.S.; methodology, M.T.G., C.S., N.L.F. and M.S.; validation, M.T.G., C.S. and M.I.G.; formal analysis, M.I.G. and N.L.F.; investigation, M.T.G. and C.S.; data curation, C.S. and M.I.G.; writing—original draft preparation, M.T.G., C.S. and M.I.G.; writing—review and editing, N.L.F. and M.S.; visualization, M.T.G., N.L.F. and M.S.; supervision, M.T.G. and M.S.; project administration, C.S. and M.I.G.; funding acquisition, M.T.G. and M.S. All authors have read and agreed to the published version of the manuscript.

Funding: This research received no external funding.

Data Availability Statement: The raw data supporting the conclusions of this article will be made available by the first/corresponding authors on request.

Acknowledgments: The proposed antenna was manufactured by Tamara Electronics Corporate. The laboratory measurements of the antenna were performed by TR Antenna Electronics Inc.

Conflicts of Interest: The authors declare no conflicts of interest.

References

1. Küçükcan, S.; Kaya, A. Dual-Band Microstrip Patch Antenna Design for Wi-Fi Applications. *Eur. J. Sci. Technol.* **2022**, *34*, 661–664. [[CrossRef](#)]
2. Gündoğdu, D.Y.; Ertay, A.O.; Enstitüsü, F.B.; Binali, E.; Üniversitesi, Y. Relatively Small, High Isolated Two Port MIMO Antenna Design for Fifth Generation Communication Systems. In Proceedings of the ELECO 2022 International Conference on Electrical and Electronics Engineering Bursa, Turkey 24–26 November 2022.

3. Fei, Z.C.; Ramli, N.; Jethi, P.L.; Sanossi, T.K.; Rahman, N.H.A. Performance Analysis of Rectangular Microstrip Patch Antenna with Different Substrate Material at 2.4 GHz for WLAN Applications. In Proceedings of the 2021 7th International Conference on Space Science and Communication (IconSpace), Selangor, Malaysia, 23–24 November 2021; pp. 46–49. [CrossRef]
4. International Telecommunication Union. Intelligent Transport Systems. In *Handbook on Land Mobile (Including Wireless Access)*, 2021st ed.; International Telecommunication Union: Geneva, Switzerland, 2021.
5. Maddio, S.; Pelosi, G.; Righini, M.; Sella, S. A compact series array for vehicular communication in the C-band. In Proceedings of the 2019 IEEE International Symposium on Antennas and Propagation and USNC-URSI Radio Science Meeting, Atlanta, GA, USA, 7–12 July 2019; pp. 1337–1338.
6. Singh, P.; Chaitanya, K.S.; Kumari, R. Microstrip patch antenna for application in intelligent transport systems. In Proceedings of the 2019 TEQIP III Sponsored International Conference on Microwave Integrated Circuits, Photonics and Wireless Networks (IMICPW), Tiruchirappalli, India, 22–24 May 2019; pp. 324–327.
7. Olaimat, M.M.; Chaouche, Y.B.; El Badawe, M.; Nedil, M.; Ramahi, O.M. Effect of Bending on Metasurface Antenna and Microstrip Patch Antenna Array. In Proceedings of the 2021 IEEE International Symposium on Antennas and Propagation and North American Radio Science Meeting, APS/URSI, Singapore, 4–10 December 2021; pp. 187–188. [CrossRef]
8. Patwary, A.B.; Abedin, S.; Hossain, M.A. Design of a ladybug shaped circular polarized microstrip antenna at 5.8 GHz as microwave power transmitter to a mav. In Proceedings of the 2019 International Conference on Electrical, Computer and Communication Engineering (ECCE), Cox’sBazar, Bangladesh, 7–9 February 2019; pp. 1–4.
9. Saini, J.; Agarwal, S.K. Design a single band microstrip patch antenna at 60 GHz millimeter wave for 5G application. In Proceedings of the 2017 International Conference on Computer, Communications and Electronics (Comptelix), Jaipur, India, 1–2 July 2017; pp. 227–230.
10. Khan, M.M.; Islam, K.; Alam Shovon, N.; Baz, M.; Masud, M. Design of a Novel 60 GHz Millimeter Wave Q-Slot Antenna for Body-Centric Communications. *Int. J. Antennas Propag.* **2021**, *2021*, 9795959. [CrossRef]
11. Roy, S.S.; Naresh, K.M.; Saha, C. Resistively loaded slotted microstrip patch antenna with controllable bandwidth. In Proceedings of the 2016 International Symposium on Antennas and Propagation, APSYM 2016, Cochin, India, 15–17 December 2016; pp. 71–74. [CrossRef]
12. Sarin, V.P.; Nassar, N.; Deepu, V.; Aanandan, C.; Mohanan, P.; Vasudevan, K. Wideband Printed Microstrip Antenna for Wireless Communications. *IEEE Antennas Wirel. Propag. Lett.* **2009**, *8*, 779–781. [CrossRef]
13. Gürsoy, G.S.; Keskin, S.E.B. Bant Çentik Karakteristiği Gösteren Ultra Geniş Bant Mikroşerit Anten Tasarımları Üzerine Bir İnceleme. *Eur. J. Sci. Technol.* **2021**, *24*, 314–320. [CrossRef]
14. Fan, T.-Q.; Jiang, B.; Liu, R.; Xiu, J.; Lin, Y.; Xu, H. A Novel Double U-Slot Microstrip Patch Antenna Design for Low-Profile and Broad Bandwidth Applications. *IEEE Trans. Antennas Propag.* **2022**, *70*, 2543–2549. [CrossRef]
15. Idris, M.K.; Sarwar, B.; Rehman, Y.; Imeci, T. Rectangular shaped microstrip patch antenna with multiple slits and slots. In Proceedings of the 2017 25th Signal Processing and Communications Applications Conference, SIU 2017, Antalya, Turkey, 15–18 May 2017. [CrossRef]
16. Shimu, N.J.; Ahmed, A. Design and performance analysis of rectangular microstrip patch antenna at 2.45 GHz. In Proceedings of the 2016 5th International Conference on Informatics, Electronics and Vision, ICIEV 2016, Dhaka, Bangladesh, 13–14 May 2016; pp. 1062–1066. [CrossRef]
17. Silalahi, L.M.; Budiayanto, S.; Silaban, F.A.; Simanjuntak, I.U.V.; Hendriasari, P.S.; Heryanto. Design of 2.4 GHz and 5.8 GHz Microstrip Antenna on Wi-Fi Network. In Proceedings of the 2020 2nd International Conference on Broadband Communications, Wireless Sensors and Powering (BCWSP), Yogyakarta, Indonesia, 28–30 September 2020; pp. 6–11. [CrossRef]
18. Venkat, K. Design of Patch Antenna for Ism Band Applications Using Cst Microwave Studio Design and Simulation of Common Feed with Double Microstrip Patch Antenna for Dual Band Satellite Applications View Project Design of Patch Antenna for Ism Band Applications Using Cst Microwave Studio. 2019. Available online: <https://www.researchgate.net/publication/360670017> (accessed on 15 December 2023).
19. *IEEE Standard for Information Technology—Telecommunications and Information Exchange between Systems—Local and Metropolitan Area Networks—Specific Requirements: Part 11: Wireless LAN Medium Access Control (MAC) and Physical Layer (PHY) Specifications: Amendment 6: Wireless Access in Vehicular Environments*; Institute of Electrical and Electronics Engineers: New York, NY, USA, 2010; ISBN 978-0-7381-6324-6.
20. Modi, A.; Sharma, V.; Rawat, A. Compact Design of Multiband Antenna for IRNSS, Satellite, 4G and 5G Applications. In Proceedings of the 5th International Conference on Computing Methodologies and Communication, ICCMC 2021, Erode, India, 8–10 April 2021; pp. 6–9. [CrossRef]
21. Narayana, B.L.; Bhavanam, S.N. Design & Simulation of Triple Frequency Triangular Patch Antenna by Using HFSS 14.0. *Int. J. Appl. Eng. Res.* **2015**, *10*, 2015.
22. Institute of Electrical and Electronics Engineers; Institute of Electrical and Electronics Engineers; Morocco Section, Jamiat al-Ḥasan al-Thani. Ecole Normale Supérieure de l’Enseignement Technique de Mohammedia, ICOA 2018 Optimization. In Proceedings of the 2018 International Conference on Optimization and Applications (ICOA), Mohammedia, Morocco, 26–27 April 2018.
23. Hassan, S.A.; Samsuzzaman, M.; Hossain, M.J.; Akhtaruzzaman, M.; Islam, T. Compact planar UWB antenna with 3.5/5.8 GHz dual band-notched characteristics for IoT application. In Proceedings of the 2017 IEEE International Conference on Telecommunications and Photonics (ICTP), Dhaka, Bangladesh, 26–28 December 2017; pp. 195–199.

24. Kumar, K.S.; Naik, B.M.; Vahini, S.; Kunooru, B.; Ramakrishna, D. Design of Miniaturized Planar Inverted F Antenna. In Proceedings of the 2022 IEEE 2nd Ukrainian Microwave Week (UkrMW), Kharkiv, Ukraine, 14–18 November 2022. [[CrossRef](#)]
25. Moradi, M.; Sharawi, M.S.; Wu, K. Analytical Model of Guided Waves in Periodically Perforated Dielectric Structure and Its Applications to Terahertz Substrate-Integrated Image Guide (SIIG). *IEEE Trans. Microw. Theory Technol.* **2023**, *71*, 4236–4246. [[CrossRef](#)]
26. Hassan, R.; Eldayasti, S.K.; Aboul-Dahab, M.A. Design of a Compact, Dual-band, and Single-Fed Patch Antenna for 5G Applications. In Proceedings of the 2023 5th International Youth Conference on Radio Electronics, Electrical and Power Engineering (REEPE), Moscow, Russia, 16–18 March 2023; pp. 1–6. [[CrossRef](#)]
27. Sifat, R.; Faruque, M.R.I.; Ramachandran, T.; Abdullah, M.; Islam, M.T.; Al-Mugren, K.S. Development of double-layer metamaterial with high effective medium ratio values for S-and C-band applications. *Heliyon* **2024**, *10*, e23851. [[CrossRef](#)] [[PubMed](#)]
28. Islam, R.; Mahbub, F.; Akash, S.B.; Prince, I.A.; Tasnim, F.; Navia, N.T. Design of a Compact Circular Patch Antenna Operating at ISM-Band for the WiMAX Communication Systems. In Proceedings of the 10th IEEE International Conference on Communication, Networks and Satellite, Comnetsat 2021, Purwokerto, Indonesia, 17–18 July 2021; pp. 358–362. [[CrossRef](#)]
29. Mahbub, F.; Islam, R.; Al-Nahiun, S.A.K.; Akash, S.B.; Hasan, R.R.; Rahman, M.A. A Single-Band 28.5GHz Rectangular Microstrip Patch Antenna for 5G Communications Technology. In Proceedings of the 2021 IEEE 11th Annual Computing and Communication Workshop and Conference, CCWC 2021, Online, 27–30 January 2021; pp. 1151–1156. [[CrossRef](#)]
30. Rahman, T.; Zhaowen, Y.; Youcef, H. A dual band monopole microstrip printed antenna for WLAN (2.4/5.2/5.8 GHz) application. In Proceedings of the ICMTCE 2013—2013 IEEE International Conference on Microwave Technology and Computational Electromagnetics, Qingdao, China, 25–28 August 2013; pp. 204–207. [[CrossRef](#)]
31. Al Ka’Bi, A. Design of a Microstrip Dual Band Fractal Antenna for Mobile Communications. In Proceedings of the 2022 IEEE International Black Sea Conference on Communications and Networking, BlackSeaCom 2022, Sofia, Bulgaria, 6–9 June 2022; pp. 85–90. [[CrossRef](#)]
32. Shafqat, A.; Tahir, F.A. Miniaturized Tapered Meandered Dual Band Dipole Antenna for WiFi 2.4/5.8 GHz Application. In Proceedings of the Progress in Electromagnetics Research Symposium-Fall (PIERS-FALL), Singapore, 19–22 November 2017.
33. Naji, D.K. Miniature Slotted Semi-Circular Dual-Band Antenna for WiMAX and WLAN Applications. *J. Electromagn. Eng. Sci.* **2020**, *20*, 115–124. [[CrossRef](#)]
34. Tak, J.; Woo, S.; Kwon, J.; Choi, J. Dual-Band Dual-Mode Patch Antenna for On-/Off-Body WBAN Communications. *IEEE Antennas Wirel. Propag. Lett.* **2016**, *15*, 348–351. [[CrossRef](#)]
35. Singh, A.K.; Abegaonkar, M.P.; Koul, S.K. Miniaturized Multiband Microstrip Patch Antenna Using Metamaterial Loading for Wireless Application. *Prog. Electromagn. Res. C* **2018**, *83*, 71–82. [[CrossRef](#)]
36. Selvam, Y.P.; Elumalai, L.; Alsath, M.G.N.; Kanagasabai, M.; Subbaraj, S.; Kingsly, S. Novel Frequency- and Pattern-Reconfigurable Rhombic Patch Antenna with Switchable Polarization. *IEEE Antennas Wirel. Propag. Lett.* **2017**, *16*, 1639–1642. [[CrossRef](#)]
37. Adamantia, C.; Locke, J.F.; Papapolymerou, J. Vehicle platform effects on performance of flexible, lightweight, and dual-band antenna for vehicular communications. *IEEE J. Microw.* **2021**, *2*, 123–133.
38. Jouini, A.; Hasnaoui, S.; Cherif, A. Comparative Study of patch antennas for C-V2x Communication. In Proceedings of the 2022 5th International Conference on Advanced Systems and Emergent Technologies (IC_ASET), Hammamet, Tunisia, 22–25 March 2022.
39. Durgun, A.C.; Balanis, C.A.; Birtcher, C.R.; Allee, D.R. Design, Simulation, Fabrication and Testing of Flexible Bow-Tie Antennas. *IEEE Trans. Antennas Propag.* **2011**, *59*, 4425–4435. [[CrossRef](#)]

Disclaimer/Publisher’s Note: The statements, opinions and data contained in all publications are solely those of the individual author(s) and contributor(s) and not of MDPI and/or the editor(s). MDPI and/or the editor(s) disclaim responsibility for any injury to people or property resulting from any ideas, methods, instructions or products referred to in the content.